Smart Materials

DOI: 10.1002/anie.201403246

Controlled Directional Water-Droplet Spreading on a High-Adhesion Surface**

Shile Feng, Sijie Wang, Longcheng Gao, Guangjun Li, Yongping Hou, and Yongmei Zheng**

Abstract: *Controlled directional spreading of a droplet on a smart high-adhesion surface was made possible by simply controlling anodic oxidation. The wettability gradient of the surface was controlled from 0.14 to 3.38° mm^{-1} by adjusting the anodic oxidation conditions. When a water droplet made contact with the substrate, the droplet immediately spread in the direction of the wettability gradient but did not move in other directions, such as those perpendicular to the gradient direction, even when the surface was turned upside down. The spreading behavior was mainly controlled by the wettability gradient. Surfaces with a V- or inverse-V-shaped wettability gradient were also formed by the same method, and two droplets on these surfaces spread either toward or away from one another as designed. This method could be used to oxidize many conductive substrates (e.g., copper, aluminum) to form surfaces with variously shaped wettability gradients. It has potential for application in microfluidic devices.*

Controlling liquid spreading on special wettable surfaces has received continued attention from the scientific community owing to promising applications in the fields of biomimetics, microfluidic devices, surface coatings, DNA microarrays, digital lab-on-a-chip systems, antifogging, fog-harvesting, inkjet printing, and thin- film lubrication.[1] Inspired by some very sophisticated strategies for the implementation of directional wetting in nature and enabled by advances in nanofabrication, researchers have achieved unidirectional liquid spreading by fabricating groove geometries with asymmetric micro- or nanostructures.[2] In all of these studies, the preparation of groove geometries is very complex, and usually a low-adhesion surface is required to drive a microdroplet. It is well-known that surface wettability is controlled not only by geometrical structure, but also by surface chemistries. In our previous studies on the cooperative effect of the Marangoni force and the temperature-responsive wettability-gradient force, directional spreading was possible on a surface with high hysteresis.[3] Although the spreading direction could be controlled by the temperature gradient, it involved the synthesis of a block copolymer, poly(methyl methylacrylate)-*b*-poly(*N*-isopropylacrylamide) (PMMA-*b*-PNIPAAm), and the applied temperature scope was limited to between 12 and 35 °C. It remains a challenge to develop simple approaches to tailoring controlled directional spreading on a surface with high hysteresis without extra limitations. Herein, we demonstrate that controlled directional spreading of a droplet on a high-adhesion surface can be made possible simply by controlling anodic oxidation. The wettability gradient on a graphite plate could be controlled from 0.14 to 3.38° mm^{-1} by adjusting the anodic oxidation conditions.

In our system, when a water droplet makes contact with the substrate, the droplet immediately spreads unidirectionally along the direction of the wettability gradient, but the droplet is held back in other directions, for example, perpendicular to the gradient direction and in directions in which the surface is homogeneous; the same spreading behavior was even observed when the surface was turned upside down. The spreading behavior is mainly controlled by the wettability gradient or contact angle (CA), and the wettability gradient has greater influence. All above observations are in good agreement with the results of a calculation of the wettability-gradient force acting on the droplet. The movement behavior of the droplets could be predicted from the values of the CA and the wettability gradient. Furthermore, a wettability gradient in the shape of a V or an upside-down V was also formed by the same method, and two droplets could spread toward or away from one another as designed.

In the present study, we improved the anodic oxidation method and also introduced a current gradient to control the extent of oxidation. A narrow-strip copper plate (not a parallel plane) parallel to the bottom of a graphite plate was used as the cathode, as shown in Figure 1 a (see the Experimental Section). For a given electrolyte composition and area of current path, the resistance of the electrolyte is proportional to the distance between the anode and cathode. Therefore, the resistance between different areas (A_1, A_2, A_3) on the graphite plate and the cathode is different ($R_1 > R_2 > R_3$; Figure 1 b). At a given voltage U, according to the Ohm law: $I = U/R$ (the resistance of the graphite plate was ignored), the current gradient would be formed during the oxidation process ($I_1 < I_2 < I_3$), as is proven by the change in the CA (see Figure S1 a,b in the Supporting Information). The wettability

[*] S. Feng, S. Wang, Prof. L. Gao, Dr. G. Li, Dr. Y. Hou, Prof. Y. Zheng
Key Laboratory of Bio-Inspired Smart Interfacial Science and Technology of the Ministry of Education
School of Chemistry and Environment, Beihang University
Beijing, 100191 (P. R. China)
E-mail: zhengym@buaa.edu.cn
houyongping09@buaa.edu.cn

[**] This research was supported by the National Key Basic Research Program of China (2013CB933000, 2010CB934700), the National Natural Science Foundation of China (21234001, 51203006, 21204002, 21004002), the Doctoral Fund of the Ministry of Education of China (20121102110035), the Specialized Research Fund for the Doctoral Program of Higher Education (20111102120049), the Beijing Natural Science Foundation (2133065), and the Aeronautical Science Foundation of China (2012ZF51065).

Supporting information for this article is available on the WWW under http://dx.doi.org/10.1002/anie.201403246.

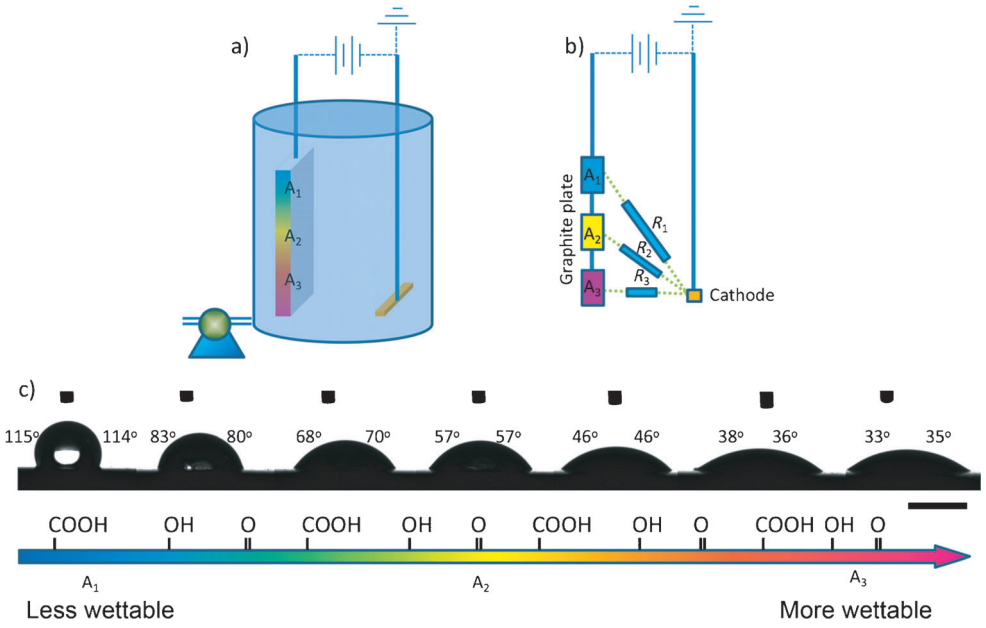

Figure 1. Schematic illustration of the formation of wettability gradients on a graphite plate and water contact angles along the gradient surface. a) Apparatus for anodic oxidation. b) Equivalent circuit diagram. To form a current gradient, a narrow-strip copper plate parallel to the bottom of the graphite plate was used as a cathode. The current-density gradient was formed as a result of the differing resistance between areas A_{1-3} and the cathode, $R_1 > R_2 > R_3$. At $t = 0$ s, a valve was used to empty the reaction vessel, thus slowly lowering the level of the solution along the graphite plate and controlling the oxidation time. The wettability gradient could be readily controlled through the current-density gradient and oxidation time. c) Photograph showing the water contact angles along the gradient surface. The photograph was combined from seven continuous photographs along the substrate because the view angle of the contact-angle-measurement system was not wide enough. The volume of the water droplets was kept at 5 μL. Scale bar: 2 mm.

gradient could be controlled from 0.14 to 1.25° mm^{-1} by adjusting the oxidation time or current. To amplify the controlling range, we used a valve attached to the bottom of the chamber to gradually empty the reaction vessel to control the oxidation time of different areas (an oxidation-time gradient was formed).[4] The bottom part of the surface would have more time to be oxidized, which is consistent with the effect of the oxidation-current gradient. As a result of the cooperative effect mentioned above, the CA changed gradually from 115 to 34° (Figure 1c), and the wettability gradient reached 3.38° mm^{-1}. Thus, we could readily adjust the wettability gradient between 0.14 and 3.38° mm^{-1} by our improved anodic oxidation method (see Figure S1).

XPS experiments were performed on different areas of the oxidized graphite plate (see Figure S2 and Table S1). The O 1s/C 1s ratio of different areas increased significantly from 0.075 to 0.36 as the distance from the top to the bottom increased. Deconvolution of the C 1s spectra gave five peaks representing graphitic carbon (peak I, 284.6 eV), carbon present in alcohol or ether groups (peak II, 286.1–286.3 eV), carbonyl groups (peak III, 287.3–287.6 eV), carboxylic acid or ester groups (peak IV, 288.4–288.9 eV), and carbon present in carbonate groups and/or adsorbed CO and CO (peak V, 290.4–2290.8 eV).[5] The spectral contribution of the carboxylic carbon peak increased from about 0.5 to 15%, and the carbonyl content increased from about 11 to 38% (see Figure S3). The C–OH peak did not increase but exhibited a small decrease. The increase in the O 1s/C 1s ratio is therefore attributed to an increase in the carboxylic and carbonyl carbon content, and the results are consistent with our design, according to which an oxidation gradient is formed, and more polar oxygen-containing groups are introduced at the bottom of the graphite plate.[5] SEM images of different areas showed little difference between different areas (see Figure S4), in accordance with the observation that the electrolyte is still clear after anodic oxidation. Therefore, we mainly ascribe the formation of a wettability gradient to the change in the surface chemical composition.

A 5 μL droplet of deionized water was placed on the sample surface, and the movement behavior was recorded by a charge coupled device (CCD) camera (Figure 2). Interestingly, the movement behavior is dependent on the CA and wettability gradient. When the contact angle and wettability gradient are very small, the droplet is pinned to the spot. When the water droplet is in contact with a surface with a large CA and wettability gradient, it spreads along the wettability gradient immediately and does not move in perpendicular directions (Figure 2a,b), thus showing unidirectional spreading behavior. In consideration of the high adhesion of the graphite plate (the water droplet does not slide down even when the graphite-plate surface is held vertically or turned upside down), the plate was turned upside down, and the droplet was dripped onto the lower surface with a bent needle. Interestingly, the droplet adhered to the lower surface and also presented unidirectional spreading behavior along the wettability gradient (Figure 2c). Thus, controlled unidirectional spreading behavior on a high-adhesion surface was realized for the first time by a straightforward anodic oxidation method.[6]

We observed the movement behavior of water droplets on different samples and recorded the spreading-distance values under different oxidation conditions (the droplet was dripped onto the middle area of each sample; Figure 3a–c). It is clear that with an increase in the oxidation time or current or volume flow, the spreading distance increased at first and then decreased remarkably, in accordance with the change in the wettability gradient. For a thorough understanding of the movement behavior of water droplets on surfaces with different wettability gradients, the forces exerted on the

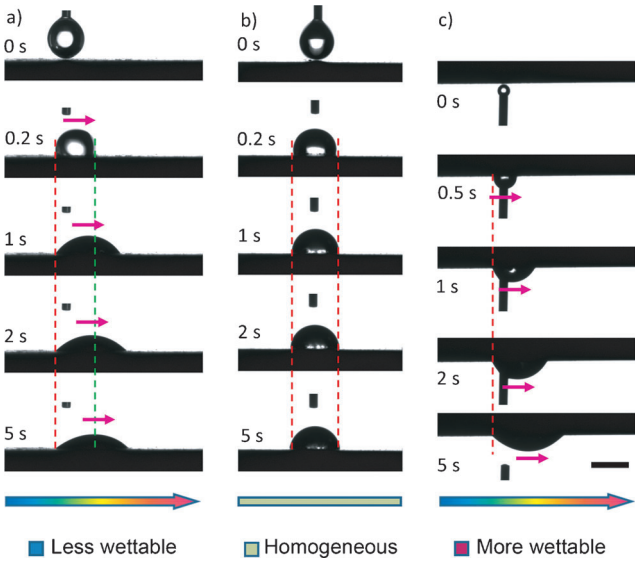

Figure 2. Water-droplet movement on the gradient surfaces. a) Spreading along the wettability gradient. b) Lack of movement in directions perpendicular to the wettability gradient. c) The graphite plate was turned upside down, and the droplet was dripped onto the lower surface. The water droplet spread along the wettability gradient and was pinned in perpendicular directions, even on the lower surface. Scale bar: 2 mm.

water droplets must be considered. There are two main forces that influence the movement of droplets: the wettability-gradient force (F_W) and the hysteresis force (F_H).

When a water droplet is contact with a surface with a wettability gradient, the two fronts along the wettability-gradient axis have different CAs. The dynamic CAs of the moving drop are, to a good approximation, equal to the Young CA in the middle of the drop base.[7] The wettability-gradient force would drive water droplets towards the more wettable region of the surface[8] and could be described as:

$$F_W = \pi R^2 \gamma \frac{d\cos\theta}{dx} = \pi R^2 \gamma \frac{d\cos\theta}{d\theta}\frac{d\theta}{dx} = \pi R^2 \gamma k \sin\theta \quad (1)$$

in which R is the base radius of the droplet, γ is the surface tension of water, θ is the position-responsive sessile CA of the water droplet, dx is the integrating variable along the wettability gradient, and k is the wettability gradient (equal to $-d\theta/dx$). For a given radius R (ca. 2 mm), the values of F_W could be plotted as a function of wettability gradient k and CA θ (Figure 3 d).

The hysteresis force (F_H) due to CA hysteresis, which is always opposite to the moving direction, is described as:[9]

$$F_H = 2R\gamma(\cos\theta_{ro} - \cos\theta_{ao}) \quad (2)$$

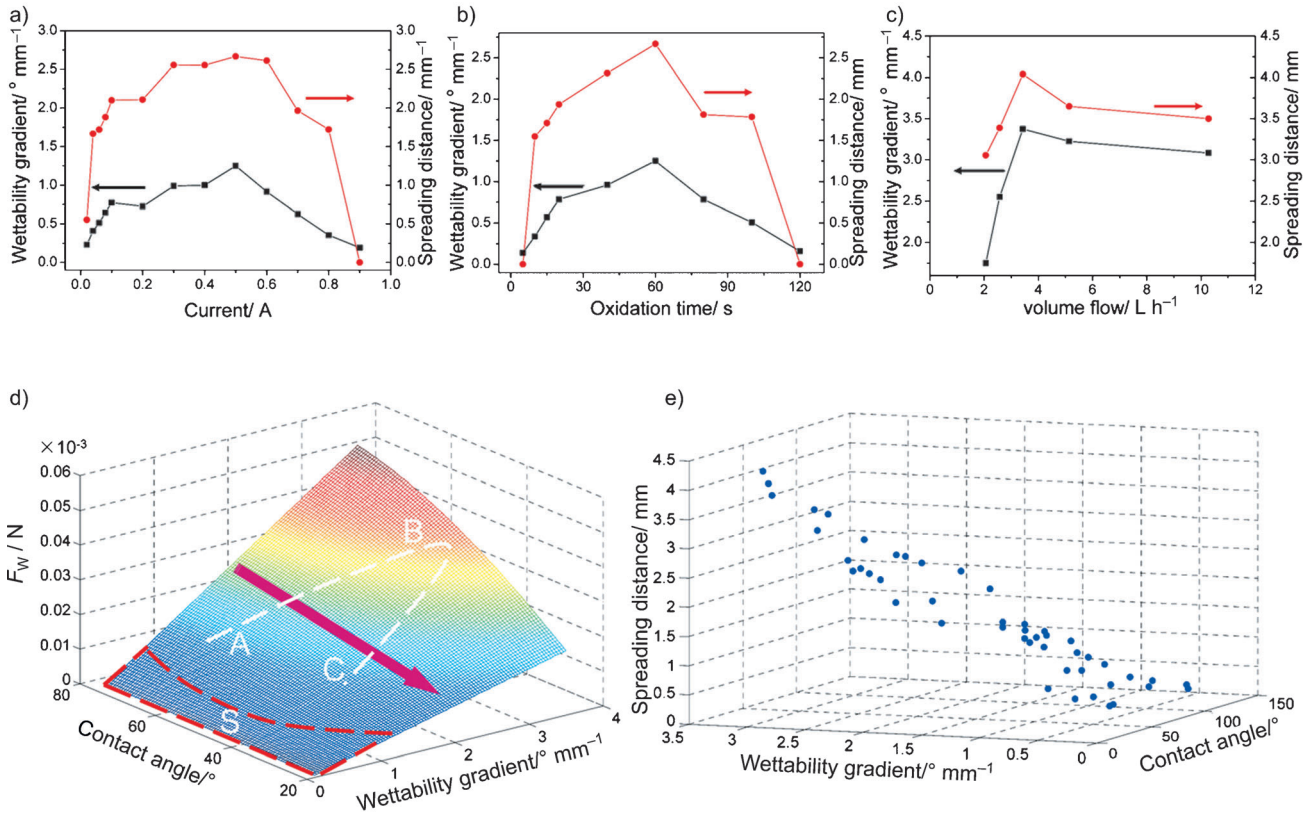

Figure 3. Influence of the oxidation conditions on the wettability gradient and spreading distance: a) current; b) oxidation time; c) volume flow. d) Calculated force (F_W) exerted on the water droplet versus the contact angle (θ) and wettability gradient (k). As the extent of oxidation increases, the F_W value should change along the route from A via B to C; that is, it should increase initially and then decrease. e) Spreading distance as a function of CA and wettability gradient.

in which θ_{ro} and θ_{ao} are the position-dependent receding and advancing CA, respectively, at the central line of the drop on the solid surface. The total force can be described as the vectorial sum of F_W and F_H.[3a,8] If the value of F_W is higher than that of F_H, the water droplet can spread on the surface.[10] Otherwise, the water droplet is pinned to the spot. Since, if it spreads, the water droplet spreads immediately when it comes in contact with the surface, it is not easy to obtain accurate values of θ_{ro} and θ_{ao}. Considering that the CA hysteresis is a direct measure of the adhesive force,[3b] we obtained the adhesive forces (along the direction of the wettability gradient) of samples with different wettability gradients in different areas to estimate the values of F_H (see Figure S5a). The results indicate that F_H increases along the direction of greater wettability and with an increasing wettability gradient. On the basis of the measurements and Equation (1), it can be roughly inferred that F_W is closely related to the wettability gradient and CA (see Figure S5b). As compared to F_W (see Figure S5b), the change in the tangent adhesive forces is very small in the range of the wettability gradient from 0.20 to 3.38° mm^{-1}. Therefore, the movement behavior of droplets may be determined from the value F_W, in good agreement with our observations that the droplet is pinned to the spot when the F_W value is below approximately 10 μN (Figure 3d, area S). This result implies that droplet spreading or pinning behavior could be predicted from the values of CA and the wettability gradient [according to Eq. (1)].

With an increase in the extent of oxidation (an increase in oxidation time and current, and a decrease in volume flow), the CA decreases gradually, and the wettability gradient increases at first and then decreases. Therefore, the F_W value should change along the route from A via B to C (Figure 3d); that is, it should increase initially and then decrease. Consequently, the spreading distance shows a peak in Figure 3a–c. We plotted the spreading distance as a function of the CA and wettability gradient (Figure 3e). Clearly, the values of spreading distance are related to the wettability gradient and the CA, and the wettability gradient has a greater influence upon the spreading distance. As a droplet spreads on the surface of the graphite plate, the wettability gradient does not change (see Figure S1), and the CA decreases gradually, which results in the reduction of F_W (Figure 3d, along the direction of arrow). When F_W is equal to F_H, the spreading behavior would be halted.

We also used a two-step method to form V- and upside-down-V-shaped wettability gradients. For the V-shaped wettability gradient, the upper part of graphite plate was first immersed in an electrolyte solution, and the lower part was immersed in nonconductive carbon tetrachloride. A valve was also used to control the oxidation time of different areas. In this way, during the anodic oxidation process, only the upper part of the plate was oxidized. After the anodic oxidation, we turned the graphite plate upside down, and the other half was oxidized in the same way (see Figure S6a). For the upside-down-V-shaped wettability gradient, first, only the lower part of the graphite plate was immersed in the electrolyte solution and oxidized during the anodic oxidation process. A valve was also used. We then turned the graphite plate upside down, and the other half was oxidized in the same way (see Figure S6b).

The desired V- or upside-down-V-shaped wettability gradient could be established by adjusting the oxidation time and current density (see Figure S7 for the change in the CA along the surface of the graphite plate). We investigated the movement behavior of droplets on surfaces with these wettability gradients (Figure 4). When two separate water droplets were dripped on a surface with a V-shaped wettability gradient, one on either side of the central line of plate, they spread toward to each other and merged quickly into one droplet. On a surface with an upside-down-V-shaped wettability gradient, although the two droplets were placed close to the central line, they could not merge into one droplet, and only spread in opposite directions (see Figure S8). When the graphite plates with the V- or upside-down-V-shaped wettability gradient were turned upside down, and the two separate water droplets were dripped onto the lower surface, similar movement behavior was still observed.

In conclusion, by simply controlling the anodic oxidation conditions, controlled directional liquid spreading was realized on a high-adhesion surface, even when the surface was

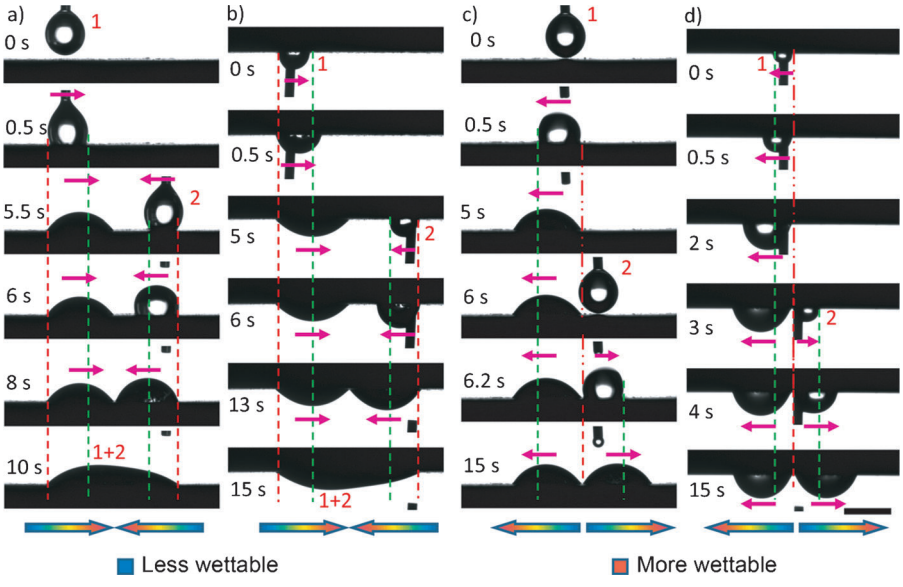

Figure 4. Water-droplet movement on surfaces with a V- or upside-down-V-shaped wettability gradient: a, b) on a surface with a V-shaped wettability gradient; c, d) on a surface with an upside-down-V-shaped wettability gradient. The results show that the two water droplets spread towards each other on a surface with a V-shaped wettability gradient and spread away from one another on a surface with an upside-down-V-shaped wettability gradient, even when the as-prepared surface is turned upside down. Scale bar: 2 mm.

turned upside down. The wettability gradient could be controlled from 0.14 to 3.38° mm^{-1} by adjusting the anodic oxidation conditions. By a two-step anodic oxidation process, a V- or upside-down-V-shaped wettability gradient was formed, and two droplets could be forced to spread by forces of a nonmechanical origin towards or away from each other as designed. This method could be used to oxidize many conductive substrates (copper, aluminum, etc.) and form surfaces with variously shaped wettability gradients. The results suggest potential applications in microfluidic devices.[11]

Experimental Section

Preparation of a graphite plate with a wettability gradient: A high-density graphite plate with a size of $30 \times 10 \times 2$ mm^3 (manufactured by Ji Xing Sheng An Co., Beijing, China; rinsed with ethanol before use) was anodically oxidized with a 0.06 M sodium hydrate (NaOH) electrolyte solution. A remarkable difference to other apparatus was that the cathode was not a parallel plane but a narrow-strip copper plate facing the bottom of the graphite plate, as shown in Figure 1 a. At a given voltage U, the current gradient is formed during the oxidation process ($I_1 < I_2 < I_3$). A valve attached to the bottom of the chamber was used to gradually empty the reaction vessel to control the oxidation time. The bottom part of the plate had more time to be oxidized, consistent with the effect of the oxidation-current gradient. Unless otherwise specified, the electrochemical process was performed at a constant current of 0.5 A with an oxidation time of 1 min. After the anodic oxidation, the graphite plate was rinsed thoroughly with freshly distilled water several times and dried at 70 °C under vacuum for 3 h, before being used as a specimen for surface analysis and the spreading test. All chemicals were analytical grade and used as received without any further treatment.

Characterization: The surface structures of the graphite plate were observed by scanning electron microscopy (SEM, Quanta FEG 250, FEI) at 10 kV. The chemical composition was analyzed by X-ray photoelectron spectroscopy (XPS; AXIS-Ultra instrument from Kratos Analytical). Water CAs were measured with an optical contact-angle meter system (OCA40 Micro, Dataphysics Instruments GmbH, Germany). A 5.0 μL droplet of deionized water was dripped onto the samples, and the static CA was determined as the average of at least five measurements. The behavior of the spreading process was recorded by a charge coupled device (CCD) camera with a time scale. Time zero was chosen to be the frame in which deposited droplets came into contact with the graphite plate. The tangent adhesion forces along the direction of the wettability gradient were measured with a surface interface tensiometer (DCA21, Dataphysics, Germany).

Received: March 12, 2014
Published online: May 12, 2014

Keywords: anodic oxidation · directional spreading · high adhesion · materials science · wettability gradients

[1] a) N.-R. Chiou, C. Lu, J. Guan, L. J. Lee, A. J. Epstein, *Nat. Nanotechnol.* **2007**, *2*, 354 – 357; b) R. Wang, K. Hashimoto, A. Fujishima, M. Chikuni, E. Kojima, A. Kitamura, M. Shimohigoshi, T. Watanabe, *Nature* **1997**, *388*, 431 – 432; c) T. N. Krupenkin, J. A. Taylor, T. M. Schneider, S. Yang, *Langmuir* **2004**, *20*, 3824 – 3827; d) Y. Hou, Y. Chen, Y. Xue, L. Wang, Y. Zheng, L. Jiang, *Soft Matter* **2012**, *8*, 11236 – 11239; e) Y. Hou, Y. Chen, Y. Xue, Y. Zheng, L. Jiang, *Langmuir* **2012**, *28*, 4737 – 4743; f) C. W. Extrand, S. I. Moon, P. Hall, D. Schmidt, *Langmuir* **2007**, *23*, 8882 – 8890; g) B. Xue, L. Gao, Y. Hou, Z. Liu, L. Jiang, *Adv. Mater.* **2013**, *25*, 273 – 277; h) W. Zhao, Y. Li, Y. Liu, W. Wie, *Ind. Eng. Chem. Res.* **2012**, *51*, 16580 – 16589.

[2] a) K.-H. Chu, R. Xiao, E. N. Wang, *Nat. Mater.* **2010**, *9*, 413 – 417; b) S. Neuhaus, N. D. Spencer, C. Padeste, *ACS Appl. Mater. Interfaces* **2012**, *4*, 123 – 130; c) D. Xia, X. He, Y.-B. Jiang, G. P. Lopez, S. R. J. Brueck, *Langmuir* **2010**, *26*, 2700 – 2706.

[3] a) Y. Hou, B. Xue, S. Guan, S. Feng, Z. Geng, X. Sui, J. Lu, L. Gao, L. Jiang, *NPG Asia Mater.* **2013**, *5*, e77; DOI: 10.1038/am.2013.70; b) W. Li, A. Amirfazli, *Adv. Mater.* **2007**, *19*, 3421 – 3422.

[4] a) S. Krämer, H. Xie, J. Gaff, J. R. Williamson, A. G. Tkachenko, N. Nouri, D. A. Feldheim, D. L. Feldheim, *J. Am. Chem. Soc.* **2004**, *126*, 5388 – 5395; b) X. Yu, Z. Wang, Y. Jiang, X. Zhang, *Langmuir* **2006**, *22*, 4483 – 4486.

[5] C. U. Pittman, Jr., W. Jiang, Z. R. Yue, S. Gardner, L. Wang, H. Toghiani, C. A. Leon y Leon, *Carbon* **1999**, *37*, 1797 – 1807.

[6] a) J. Z. Chen, S. M. Troian, A. A. Darhuber, S. Wagner, *J. Appl. Phys.* **2005**, *97*, 014906; b) V. Pratap, N. Moumen, R. S. Subramanian, *Langmuir* **2008**, *24*, 5185 – 5193; c) R. H. Farahi, A. Passian, T. L. Ferrell, T. Thundat, *Appl. Phys. Lett.* **2004**, *85*, 4237 – 4239.

[7] S. Daniel, M. K. Chaudhury, *Langmuir* **2002**, *18*, 3404 – 3407.

[8] H. Bai, X. Tian, Y. Zheng, J. Ju, Y. Zhao, L. Jiang, *Adv. Mater.* **2010**, *22*, 5521 – 5525.

[9] E. Lorenceau, D. Quéré, *J. Fluid Mech.* **2004**, *510*, 29 – 45.

[10] a) H. P. Greenspan, *J. Fluid Mech.* **1978**, *84*, 125 – 143; b) F. Brochard, *Langmuir* **1989**, *5*, 432 – 438.

[11] a) Y. Hou, L. Gao, S. Feng, Y. Xue, L. Jiang, Y. Zheng, *Chem. Commun.* **2013**, *49*, 5253 – 5255; b) B. Han, W. Zhao, X. Qin, Y. Li, Y. Sun, W. Wei, *Catal. Commun.* **2013**, *33*, 38 – 41; c) C. D. Bain, G. M. Whitesides, *Angew. Chem.* **1989**, *101*, 522 – 528; *Angew. Chem. Int. Ed. Engl.* **1989**, *28*, 506 – 512; d) S. Wang, X. Feng, J. Yao, L. Jiang, *Angew. Chem.* **2006**, *118*, 1286 – 1289; *Angew. Chem. Int. Ed.* **2006**, *45*, 1264 – 1267.

